



Cite this: *Chem. Sci.*, 2021, **12**, 8811-8816

All publication charges for this article have been paid for by the Royal Society of Chemistry

Received 29th March 2021

Accepted 25th May 2021

DOI: 10.1039/d1sc01764k

[rsc.li/chemical-science](http://rsc.li/chemical-science)

## Introduction

Induction of nonracemic screw-sense in dynamic helical macromolecular structures has gained ever-increasing interest<sup>1</sup> because unique chiral functions of dynamic nonracemic helical macromolecules have rapidly been developed in chiral separation,<sup>2</sup> chiral detection,<sup>3</sup> selective emission/reflection of circularly polarized light,<sup>4,5</sup> and asymmetric catalysis.<sup>6</sup> Recent efforts have enabled the use of external chiral sources for the induction of helical macromolecules that have no covalently bonded chiral groups.<sup>7-10</sup> Although the use of covalently bonded chiral side chains has been a quite robust strategy to form nonracemic helical main chain conformations,<sup>11</sup> the utilization of external chiral additives as sources of chirality is quite advantageous because it allows escaping from the tedious and costly synthesis of monomers containing chiral groups.

Chiral additives that interact with polymer chains through dynamic covalent bonds,<sup>7</sup> ionic interactions,<sup>8</sup> hydrogen bonding,<sup>9</sup> and host-guest interactions<sup>10</sup> have been used to shift the equilibrium between right- and left-handed helical conformations. Particular interest is currently focused on the utilization of weak nonbonding interactions such as dipole-dipole

and dispersion interactions for the induction of single-handed screw-sense.<sup>12</sup> Even though the polymer has no specific receptor sites to interact with chiral additives, unfunctionalized chiral molecules including chiral hydrocarbons and haloalkanes allow inducing biased screw-sense to the polymer main chain. This induction mode is remarkable in that significant screw-sense induction has been achieved despite the weak nondirectional molecular interactions. Macromolecular scaffolds allow amplifying such small energy differences per monomer units in large macromolecular scaffolds.<sup>13</sup> Through this mode of chirality induction, detection of “hidden” chirality of saturated hydrocarbons with quaternary stereocenters has been enabled.<sup>3</sup>

Utilization of a chiral nonbonding interaction allowed us to induce single-handed screw-sense to virtually achiral poly(quinolazine-2,3-diyli)s (PQX hereafter) using chiral solvents including limonene.<sup>14,15</sup> Application of these macromolecules as a chiral ligand in highly enantioselective asymmetric catalysis has been demonstrated as the first example for the use of chiral solvent as a source of chirality in asymmetric catalysis.<sup>16</sup> In the system, the nonbonding interactions, including dispersion forces, between chiral solvent and the backbone of PQX may play a crucial role in determining the position of equilibrium between right- and left-handed helical conformations. Although the details of their molecular interaction await further clarification, the scope of chiral guests is important practically to find more applications of this unique phenomenon. Particularly important is the utilization of naturally occurring chiral feedstocks as chiral additives and reduction of their loading amounts. In this paper, we screened natural amino acid derivatives as new chiral additives for induction of single-handed screw-sense, which leads to an asymmetric Suzuki-Miyaura

Department of Synthetic Chemistry and Biological Chemistry, Graduate School of Engineering, Kyoto University, Katsura, Nishikyo-ku, Kyoto 615-8510, Japan. E-mail: [suginome@sbchem.kyoto-u.ac.jp](mailto:suginome@sbchem.kyoto-u.ac.jp); [nagata@icredd.hokudai.ac.jp](mailto:nagata@icredd.hokudai.ac.jp)

† Electronic supplementary information (ESI) available. See DOI: 10.1039/d1sc01764k

‡ Current address: Institute for Chemical Reaction Design and Discovery (WPI-ICReDD), Hokkaido University, Kita 21, Nishi 10, Kita-ku, Sapporo, Hokkaido 001-0021, Japan.



coupling reaction in the presence of a virtually achiral macro-molecular phosphine ligand along with a small amount of fully protected amino acids such as Ac-*L*-Pro-OMe.

## Results and discussion

To test the ability of protected amino acids in screw-sense induction, circular dichroism (CD) spectra of PQX *n*-mer (**PQX(n)**) bearing *n*-propoxymethyl side chains in various achiral solvents with the protected amino acids were measured (Scheme 1). Firstly, CD spectra of **PQX(100)** in THF containing 16 enantiopure Boc-protected amino acid methyl esters were compared (amino acid/THF = 10 : 90 (mol/mol)). All spectra showed the same CD signals with varied intensities and signs (see the ESI†). The signs and intensities of the CD signal (dissymmetry factor; *g* value) at 366–371 nm at 293 K are summarized in Table 1. For the sake of comparison, when used as a chiral additive in THF (11 mol%), (*R*)-limonene afforded *g*<sub>abs</sub> of  $0.53 \times 10^{-3}$ , which corresponds roughly to 20–25% screw-sense excess (se) (entry 0).

The proline derivative showed the most efficient induction, leading to the formation of left-handed (*M*) helix with se higher than 50% (entry 1). A six-membered ring derivative Boc-Pip-OMe (*D*-isomer) and *L*-Ala also showed efficient screw-sense induction to the same direction as *L*-Pro in terms of the relationship between the absolute configuration of the additives and the induced screw sense. Indeed, the observed screw-sense induction was significantly higher than the induction by (*R*)-limonene (entry 0). The majority of the *L*- and *D*-amino acid derivatives induced *M*- and *P*-helical conformation, respectively, with varied degrees of screw-sense induction (entries 1–12). However, four of the tested *L*-amino acids including the leucine and asparagine derivatives (entries 15 and 16) induced right-handed (*P*) helical conformation albeit with low screw sense excesses (entries 13–16). No clear relationship was found between the sense/degree of screw-sense induction and the structure of the amino acid derivatives.

**Table 1** CD intensities of **PQX(100)** in THF in the presence of Boc-protected amino acid methyl esters<sup>a</sup>

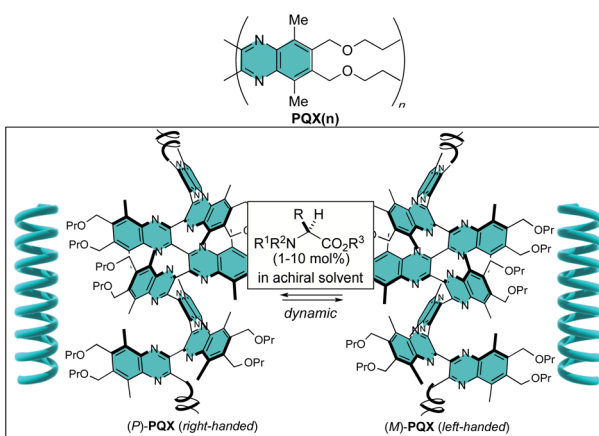
| Entry | Chiral additives                   | CD intensities ( <i>g</i> <sub>abs</sub> /10 <sup>-3</sup> ) <sup>b</sup> |
|-------|------------------------------------|---|
| 0     | ( <i>R</i> )-limonene <sup>c</sup> | +0.53 ( <i>P</i> )  |
| 1     | Boc- <i>L</i> -Pro-OMe             | -1.16 ( <i>M</i> )  |
| 2     | Boc- <i>D</i> -Pip-OMe             | +0.80 ( <i>P</i> )  |
| 3     | Boc- <i>L</i> -Ala-OMe             | -0.80 ( <i>M</i> )  |
| 4     | Boc- <i>L</i> -Thr-OMe             | -0.63 ( <i>M</i> )  |
| 5     | Boc- <i>L</i> - <i>t</i> -Leu-OMe  | -0.35 ( <i>M</i> )  |
| 6     | Boc- <i>L</i> -Glu(OMe)-OMe        | -0.34 ( <i>M</i> )  |
| 7     | Boc- <i>L</i> -Ile-OMe             | -0.28 ( <i>M</i> )  |
| 8     | Boc- <i>L</i> -Asn-OMe             | -0.22 ( <i>M</i> )  |
| 9     | Boc- <i>L</i> -Tyr-OMe             | -0.15 ( <i>M</i> )  |
| 10    | Boc- <i>L</i> -Ser-OMe             | -0.28 ( <i>M</i> )  |
| 11    | Boc- <i>L</i> -Gln-OMe             | -0.19 ( <i>M</i> )  |
| 12    | Boc- <i>L</i> -Val-OMe             | -0.07 ( <i>M</i> )  |
| 13    | Boc- <i>L</i> -Phe-OMe             | +0.08 ( <i>P</i> )  |
| 14    | Boc- <i>L</i> -Cys-OMe             | +0.10 ( <i>P</i> )  |
| 15    | Boc- <i>L</i> -Asp(OMe)-OMe        | +0.29 ( <i>P</i> )  |
| 16    | Boc- <i>L</i> -Leu-OMe             | +0.18 ( <i>P</i> )  |

<sup>a</sup> In THF containing the amino acid (AA) derivatives (molar ratio of AA derivatives and THF = 10 : 90) with **PQX(100)** (ca.  $7 \times 10^{-4}$  M) at 293 K.

<sup>b</sup>  $\Delta\varepsilon/\varepsilon$  at 367–371 nm (293 K). <sup>c</sup> 11 : 89 molar ratio of limonene and THF.

We then evaluated the effect of protective groups of proline on the screw-sense induction (Table 2). In terms of the groups at the C-termini, protection with ester was found to be more effective than amide or acid functionality (entries 1–5). Among a series of esters, methyl esters showed the highest induction. In terms of *N*-protection, trifluoroacetamide and acetamide showed a much more efficient induction of *M*-helical sense (entries 8 and 9, 80–85% se) than did the others.

We found a strong effect of solvent on the screw-sense induction to **PQX(30)** with TFAC-*L*-Pro-OMe (Fig. 1, red bars). In comparison to THF used in the above measurements, significantly weaker induction was obtained in chloroform. By contrast, *t*-butyl methyl ether (MTBE) showed much more effective induction than did THF. This trend was maintained in the induction to **PQX(30)** with Ac-*L*-Pro-OMe (Fig. 1, blue bars). This result suggests that chloroform has a strong nonbonding



**Scheme 1** Two enantiomeric (*P*- and *M*-) conformations of achiral PQX, of which equilibrium is shifted by *N*-protected amino acid esters used as additives in an achiral solvent.

**Table 2** CD intensities of **PQX(100)** in THF in the presence of protected proline and leucine derivatives<sup>a</sup>

| Entry | Amino acid derivatives   | CD intensities ( <i>g</i> <sub>abs</sub> /10 <sup>-3</sup> ) <sup>b</sup> |
|-------|--|---|
| 1     | Boc- <i>L</i> -Pro-OMe   | -1.16 ( <i>M</i> )  |
| 2     | Boc- <i>L</i> -Pro-NH <sub>2</sub>                             | -0.29 ( <i>M</i> )  |
| 3     | Boc- <i>L</i> -Pro-OH  | -0.52 ( <i>M</i> )  |
| 4     | Boc- <i>L</i> -Pro-OEt   | -0.79 ( <i>M</i> )  |
| 5     | Boc- <i>L</i> -Pro-O- <i>n</i> -C <sub>6</sub> H <sub>13</sub> | -1.01 ( <i>M</i> )  |
| 6     | Cbz- <i>L</i> -Pro-OMe   | -1.08 ( <i>M</i> )  |
| 7     | Piv- <i>L</i> -Pro-OMe   | -1.31 ( <i>M</i> )  |
| 8     | Ac- <i>L</i> -Pro-OMe  | -1.75 ( <i>M</i> )  |
| 9     | TFAC- <i>L</i> -Pro-OMe  | -1.64 ( <i>M</i> )  |

<sup>a</sup> In THF containing the amino acid (AA) derivatives (molar ratio: 90 : 10) with **PQX(100)** (ca.  $7 \times 10^{-4}$  M) at 293 K. <sup>b</sup>  $\Delta\varepsilon/\varepsilon$  at 367–371 nm (293 K).



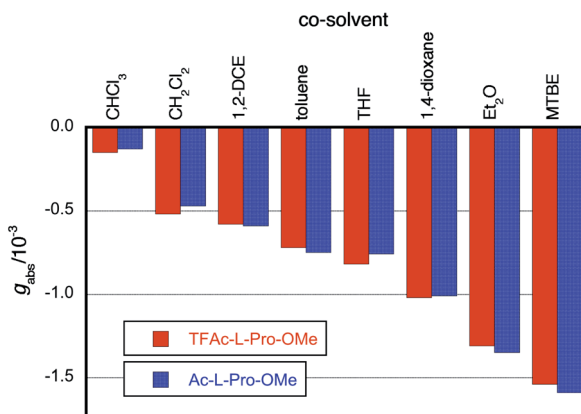


Fig. 1 CD intensities ( $g_{\text{abs}}$  at 367–371 nm at 293 K) of PQX(30) in various solvents in the presence of TFAc-L-Pro-OMe and Ac-L-Pro-OMe (10 mol% in the solvents).

interaction with PQX, thereby preventing interaction of the chiral guests with PQX, while MTBE has a weak interaction with PQX, thus maximizing the screw-sense induction. Although we cannot exclude the other possibility where the chiral additive anyhow interacts with polymer preferentially over the solvent to form “supramolecular complex”, of which screw-sense is steered by solvent effect. However, our NMR measurements of Ac-L-Pro-OMe in the presence of PQX(100) in different solvents revealed that the chemical shifts of Ac-L-Pro-OMe sharply depends on solvent (Fig. 2(A)). Whereas no apparent change of the chemical shift was observed in CHCl<sub>3</sub> and toluene, appreciable change was observed in THF, dioxane, and MTBE. In particular, remarkable change of chemical shift was observed in MTBE. This result may support the former assumption that there is competitive interaction by chiral additives and achiral

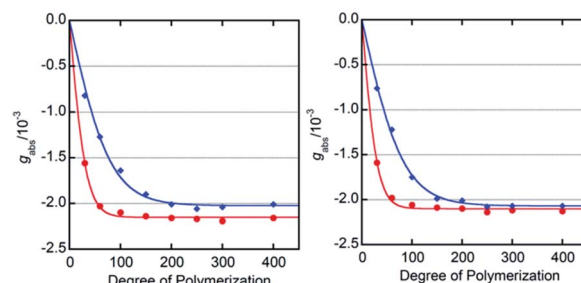


Fig. 3 CD intensities ( $g_{\text{abs}}$  at 367–371 nm at 293 K) of PQX(n) (ca.  $7 \times 10^{-4}$  M based on monomer units,  $n = 30, 60, 100, 150, 200, 250, 300$ , and 400) in THF (blue diamonds) and MTBE (red circles) in the presence of TFAc-L-Pro-OMe (left) and Ac-L-Pro-OMe (right) (10 mol%).

solvent. In the <sup>1</sup>H NMR measurements of Ac-L-Pro-OMe, all the signals of Ac-L-Pro-OMe were up-field shifted in the presence of PQX(100). The  $\Delta\delta$  observed in cyclohexane-*d*<sub>12</sub>, in which the up-field shift was even more pronounced, are shown in Fig. 2(B). It should be noted that the hydrophobic region, *i.e.*, the Ac methyl group and ring methylenes, of the major *anti*-conformer of Ac-L-Pro-OMe showed larger change of chemical shifts than did its other part, which contains polar carbonyl oxygens. Although this observation still gives no clear information on the nature of the nonbonding interaction, it is likely that the hydrophobic region of Ac-L-Pro-OMe is more favorably incorporated into the backbone of PQX, of which quinoxaline rings may bring about the observed up-field shift in the NMR measurements.

We determined the energy profile of the *P/M* equilibria in THF and MTBE in the presence of Ac- and TFAc-L-Pro-OMe (10 mol%) by measuring the CD spectra of PQX(n) with

| solvent                                   | $\Delta\delta$ (ppb) |     |            |     |
|---|----------------------|-----|------------|-----|
|   | <i>anti</i>          |     | <i>syn</i> |     |
|   | Ac                   | OMe | Ac         | OMe |
| CDCl <sub>3</sub>                         | -1                   | -1  | 0          | -1  |
| toluene- <i>d</i> <sub>8</sub>            | -1                   | 0   | -1         | -1  |
| THF- <i>d</i> <sub>8</sub>                | -4                   | -1  | -2         | -3  |
| 1,4-dioxane- <i>d</i> <sub>8</sub>        | -6                   | -2  | -2         | -4  |
| MTBE/C <sub>6</sub> D <sub>12</sub> (4/1) | -27                  | -10 | -8         | -13 |

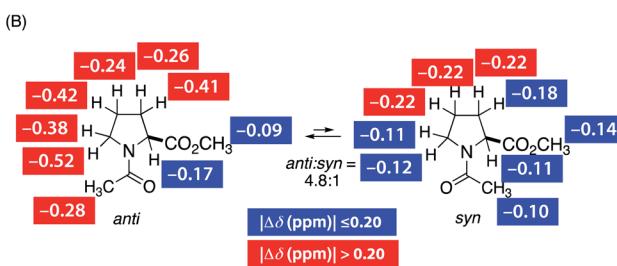


Fig. 2 Shift of <sup>1</sup>H NMR chemical shifts ( $\Delta\delta$ ) of *anti* (major) and *syn* (minor) conformers of Ac-L-Pro-OMe by the effect of PQX(100) (A) at methyl groups in various solvents at 19.4 °C ([PQX(100)] = ca.  $5.0 \times 10^{-2}$  M; [Ac-L-Pro-OMe] = ca.  $1.3 \times 10^{-3}$  M) and (B) at their all protons in cyclohexane-*d*<sub>12</sub> at 8.5 °C ([PQX(100)] = ca.  $1.6 \times 10^{-1}$  M; [Ac-L-Pro-OMe] = ca.  $5.7 \times 10^{-3}$  M).

Table 3 Summary of calculated helix stabilization energies  $\Delta G_h$  and maximum CD intensities ( $g_{\text{max}}$ ) for PQX(n) under various conditions at 293 K

| Entry | Chiral additive (mol%) | Solvent | $\Delta G_h$ (kJ mol <sup>-1</sup> ) | $g_{\text{max}}/10^{-3}$ |
|-------|------------------------|---------|--------------------------------------|--------------------------|
| 1     | (R)-Limonene (100)     | None    | 0.104                                | +2.37 (P)                |
| 2     | TFAc-L-Pro-OMe (10)    | THF     | 0.060                                | -2.02 (M)                |
| 3     | TFAc-L-Pro-OMe (10)    | MTBE    | 0.148                                | -2.15 (M)                |
| 4     | Ac-L-Pro-OMe (10)      | THF     | 0.059                                | -2.07 (M)                |
| 5     | Ac-L-Pro-OMe (10)      | MTBE    | 0.157                                | -2.10 (M)                |

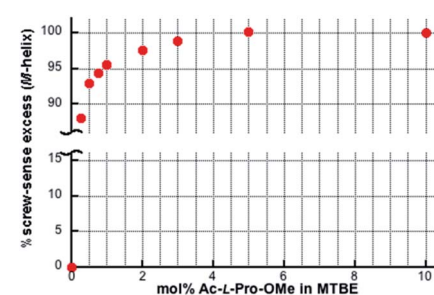
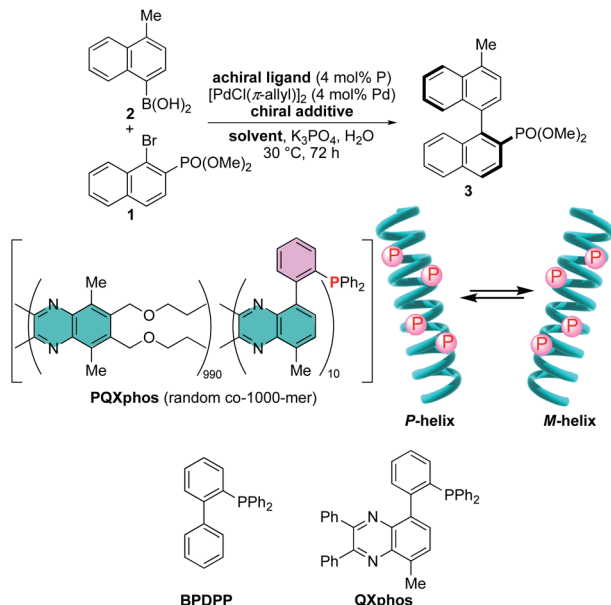


Fig. 4 Screw-sense excesses of PQX(1000) (ca.  $7 \times 10^{-4}$  M based on monomer units) in MTBE in the presence of Ac-L-Pro-OMe with varied concentrations.



Scheme 2 Asymmetric Suzuki–Miyaura coupling in the presence of achiral phosphine ligands including **PQXphos** with chiral additives.

different polymerization degrees ( $n = 30\text{--}400$ ), which were selectively synthesized using living polymerization (Fig. 3). The plot of CD intensities against polymerization degrees showed that higher screw-sense induction was achieved with increase in polymerization degree. The curve fitting according to Green's theory<sup>13</sup> brings about the energy difference between *M*- and *P*-helices per unit ( $\Delta G_h$ ) of  $0.16\text{ kJ mol}^{-1}$  for Ac-*L*-Pro-OMe in MTBE (Table 3, entry 5). The  $\Delta G_h$  with Ac-*L*-Pro-OMe in MTBE is significantly higher than that in pure limonene, even though the amino acid additives are used in a small quantity. Even the use of  $0.25\text{ mol\%}$  Ac-*L*-Pro-OMe in MTBE allows the induction of *M*-helix with  $88\text{ se}$  to **PQX(1000)** (Fig. 4).

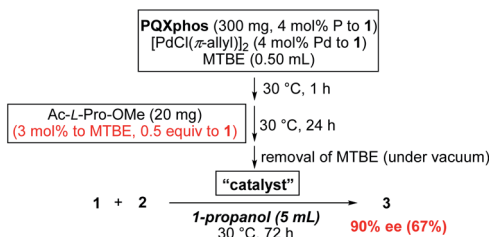
We then sought the possibility of application of the particular helix induction in asymmetric catalysis, by taking Suzuki–Miyaura coupling of naphthyl bromide **1** with naphthylboronic acid **2** as a model reaction (Scheme 2).<sup>6b,14,17,18</sup> Achiral **PQXphos** (1000-mer) containing diphenylphosphino groups was used as a ligand. In advance, we confirmed that no product was obtained in the absence of **PQXphos** and that racemic coupling product was obtained in the absence of a chiral additive (Table 4, entries 1 and 2). Use of  $10\text{ mol\%}$  (*R*)-limonene as a chiral additive resulted in the formation of the coupling product **3** with  $43\text{ ee}$  (entry 3). TFAc-*L*-Pro-OMe was then used as a chiral additive in THF (1 : 9 molar ratio) in asymmetric Suzuki–Miyaura coupling. We observed the formation of **3** with  $92\text{ ee}$ , although the chemical yield was disappointingly low (entry 4). The use of achiral low-molecular weight phosphines such as **BPDPP** and **QXphos** in the presence of TFAc-*L*-Pro-OMe resulted in the formation of racemates with low chemical yields (entries 5 and 6). These results suggested that the chiral reaction space is not formed directly by the chiral additive through its coordination to palladium metal, but rather, created by screw-sense induction to the polymer backbone. The results also suggested that the added TFAc-*L*-Pro-OMe significantly inhibited the coupling reactions. When we reduced the loading of the chiral additive in the reactions with **PQXphos**, the reaction yields were improved, but enantioselectivity decreased significantly (entries 7–10). In MTBE, we observed even stronger inhibition of the reaction, even though the higher enantioselectivity was obtained (entry 11). We found that the degree of reaction inhibition was improved significantly with use of Ac-*L*-Pro-OMe in MTBE, which afforded **3** in much better yield with  $95\text{ ee}$  (entry 12). By reducing the loading of the chiral additive to  $1\text{ mol\%}$  in MTBE, we obtained higher chemical yields without affecting the enantioselectivity significantly (entries 13–15). The use of enantiomeric Ac-*D*-Pro-OMe as a chiral guest led to the formation of an enantiomeric

Table 4 Asymmetric Suzuki–Miyaura coupling using chiral additive as a source of chirality<sup>a</sup>

| Entry | Chiral additive (mol% in solvent) | Ligand         | Solvent | Yield/% | ee/%   |
|-------|-----------------------------------|----------------|---------|---------|--------|
| 1     | None                              | <b>PQXphos</b> | THF     | 63      | 0      |
| 2     | TFAc- <i>L</i> -Pro-OMe (10)      | None           | THF     | 0       | —      |
| 3     | ( <i>R</i> )-Limonene (10)        | <b>PQXphos</b> | THF     | 57      | 43     |
| 4     | TFAc- <i>L</i> -Pro-OMe (10)      | <b>PQXphos</b> | THF     | 16      | 92     |
| 5     | TFAc- <i>L</i> -Pro-OMe (10)      | <b>BPDPP</b>   | THF     | 12      | 0      |
| 6     | TFAc- <i>L</i> -Pro-OMe (10)      | <b>QXphos</b>  | THF     | 17      | 0      |
| 7     | TFAc- <i>L</i> -Pro-OMe (7)       | <b>PQXphos</b> | THF     | 27      | 87     |
| 8     | TFAc- <i>L</i> -Pro-OMe (5)       | <b>PQXphos</b> | THF     | 49      | 84     |
| 9     | TFAc- <i>L</i> -Pro-OMe (3)       | <b>PQXphos</b> | THF     | 49      | 54     |
| 10    | TFAc- <i>L</i> -Pro-OMe (1)       | <b>PQXphos</b> | THF     | 55      | 36     |
| 11    | TFAc- <i>L</i> -Pro-OMe (5)       | <b>PQXphos</b> | MTBE    | 10      | 95     |
| 12    | Ac- <i>L</i> -Pro-OMe (10)        | <b>PQXphos</b> | MTBE    | 48      | 95     |
| 13    | Ac- <i>L</i> -Pro-OMe (5)         | <b>PQXphos</b> | MTBE    | 60      | 91     |
| 14    | Ac- <i>L</i> -Pro-OMe (3)         | <b>PQXphos</b> | MTBE    | 64      | 91     |
| 15    | Ac- <i>L</i> -Pro-OMe (1)         | <b>PQXphos</b> | MTBE    | 71      | 87     |
| 16    | Ac- <i>D</i> -Pro-OMe (3)         | <b>PQXphos</b> | MTBE    | 62      | 92 (S) |

<sup>a</sup> Standard reaction conditions: **PQXphos** (30 mg,  $1.0\text{ }\mu\text{mol}$  P) and  $[\text{PdCl}(\pi\text{-allyl})_2]$  ( $1.0\text{ }\mu\text{mol}$  Pd) were stirred in a solvent (0.50 mL) at  $30\text{ }^\circ\text{C}$  for 1 h. Chiral additive was added to the mixture, which was stirred at  $30\text{ }^\circ\text{C}$  for 24 h. The bromide **1** (0.025 mmol), the boronic acid **2** (0.050 mmol),  $\text{K}_3\text{PO}_4$  (0.075 mmol), and  $\text{H}_2\text{O}$  (25 mL) were added, and the resultant mixture was stirred at  $30\text{ }^\circ\text{C}$  for 72 h.





**Scheme 3** Asymmetric Suzuki-Miyaura coupling with the use of a substoichiometric amount of chiral nonbonding guest.

(*S*)-coupling product under the same reaction conditions (entry 16).

We tried to reduce the amount of chiral additives, keeping the concentration of chiral additive at 3 mol% in MTBE, but increasing the concentration of **PQXphos** in the helix induction step. In a 10-fold reaction scale, Ac-L-Pro-OMe (20 mg) and MTBE (0.50 mL, 3 : 97 molar ratio) were used in the equilibration step (Scheme 3). The amount of Ac-L-Pro-OMe corresponds to 0.5 equiv. of **1** and 0.13 equiv. of monomer units of **PQXphos**. After the removal of MTBE used in the equilibration, 1-propanol (5 mL) was added as a reaction solvent to the solid catalyst before starting the reaction. The heterogeneous reaction, in which the catalyst was hardly dissolved, afforded **3** with 90% ee in 67% yield. By contrast, when the reaction was carried out in MTBE without switching the solvent to 1-propanol, **3** was obtained with 68% ee (73% yield). These results suggested that homochiral *M*-helix sense was induced in the equilibration step at high concentration with a substoichiometric amount of Ac-L-Pro-OMe, and that the induced helix was maintained during the progress of the reaction in the solid state using 1-propanol as a reaction solvent.

## Conclusions

We found that protected amino acids enable the screw-sense induction to virtually achiral poly(quinoxaline-2,3-diy)s (**PQX**) that have no chiral group or receptor site. The induction power of proline derivatives such as Ac-Pro-OMe and TFAC-Pro-OMe were significantly stronger than limonene, which previously showed the most powerful screw-sense induction among the chiral solvents. A significant effect of achiral solvent was noted: ether solvents, particularly MTBE, resulted in better screw-sense induction than did halogenated solvents such as chloroform, probably because of weaker interaction with **PQX**. Upon using achiral **PQXphos** containing diphenylphosphino coordinating groups, asymmetric Suzuki-Miyaura coupling proceeded with high enantioselectivities with up to 95% ee in the presence of protected proline derivatives as a sole chiral source. For use in catalysis, Ac-Pro-OMe was found to be most effective, while TFAC-Pro-OMe significantly retarded the catalysis. These results clearly demonstrate that nonbonding interaction between the chiral additives and dynamic helical polymer can serve as an effective driving force to shift the equilibrium of helical conformations, leading to highly enantioselective asymmetric catalysis.

## Data availability

The datasets supporting this article have been uploaded as part of the supplementary material.

## Author contributions

The study is conceptualized and supervised by M. S. and Y. N. Experiments are conducted by S. I., T. F., and N. A. with initial support by R. T. The manuscript is written by M. S. and checked by all the co-authors.

## Conflicts of interest

There are no conflicts to declare.

## Acknowledgements

This work was supported by JSPS KAKENHI on Innovative Areas (Grant Number JP15H05811 in Precisely Designed Catalysts with Customized Scaffolding), KAKENHI (S) (Grant Number 20H05674), KAKENHI (A) (Grant Number 20H00377), and JST CREST (Grant Number JPMJCR14L1 in Establishment of Molecular Technology toward the Creation of New Function).

## Notes and references

- (a) E. Yashima, K. Maeda, H. Iida, Y. Furusho and K. Nagai, *Chem. Rev.*, 2009, **109**, 6102–6211; (b) E. Yashima, N. Ousaka, D. Taura, K. Shimomura, T. Ikai and K. Maeda, *Chem. Rev.*, 2016, **116**, 13752–13990.
- (a) K. Shimomura, T. Ikai, S. Kanoh, E. Yashima and K. Maeda, *Nat. Chem.*, 2014, **6**, 429–434; (b) D. Hirose, A. Isobe, E. Quiñoá, F. Freire and K. Maeda, *J. Am. Chem. Soc.*, 2019, **141**, 8592–8598.
- K. Maeda, D. Hirose, N. Okoshi, K. Shimomura, Y. Wada, T. Ikai, S. Kanoh and E. Yashima, *J. Am. Chem. Soc.*, 2018, **140**, 3270–3276.
- Chirality-switchable emission of circularly polarized luminescence: T. Nishikawa, Y. Nagata and M. Sugino, *ACS Macro Lett.*, 2017, **6**(4), 431–435.
- Chirality-switchable reflection of circularly polarized light: (a) Y. Nagata, K. Takagi and M. Sugino, *J. Am. Chem. Soc.*, 2014, **136**, 9858–9861; (b) Y. Nagata, M. Uno and M. Sugino, *Angew. Chem., Int. Ed.*, 2016, **55**, 7126–7130. For the seminal works on the use of helical polymers for CPL reflection, see: ; (c) G. Maxein, H. Keller, B. M. Novak and R. Zentel, *Adv. Mater.*, 1998, **10**, 341–345; (d) J. Watanabe, H. Kamee and M. Fujiki, *Polym. J.*, 2001, **33**, 495–497; (e) K. E. Shopsowitz, H. Qi, W. Y. Hamad and M. J. MacLachlan, *Nature*, 2010, **468**, 422–425; (f) M. K. Khan, M. Giese, M. Yu, J. A. Kelly, W. Y. Hamad and M. J. MacLachlan, *Angew. Chem., Int. Ed.*, 2013, **52**, 8921–8924.
- (a) T. Yamamoto, T. Yamada, Y. Nagata and M. Sugino, *J. Am. Chem. Soc.*, 2010, **132**, 7899–7901; (b) T. Yamamoto, Y. Akai, Y. Nagata and M. Sugino, *Angew. Chem., Int.*



*Ed.*, 2011, **50**, 8844–8847; (c) Y. Akai, T. Yamamoto, Y. Nagata, T. Ohmura and M. Suginome, *J. Am. Chem. Soc.*, 2012, **134**, 11092–11095; (d) T. Yamamoto, R. Murakami and M. Suginome, *J. Am. Chem. Soc.*, 2017, **139**, 2557–2560; (e) Y. Yoshinaga, T. Yamamoto and M. Suginome, *J. Am. Chem. Soc.*, 2020, **142**, 18317–18323; (f) T. Yamamoto, T. Takahashi, R. Murakami, N. Ariki and M. Suginome, *Bull. Chem. Soc. Jpn.*, 2021, **94**, 943–949. For the seminal work on the use of static helical polymers as chiral catalysts, see: ; (g) M. Reggelin, M. Schultz and M. Holzbach, *Angew. Chem., Int. Ed.*, 2002, **41**, 1614–1617; (h) G. Roelfes and B. L. Feringa, *Angew. Chem., Int. Ed.*, 2005, **44**, 3230–3232; (i) A. J. Boersma, R. P. Megens, B. L. Feringa and G. Roelfes, *Chem. Soc. Rev.*, 2010, **39**, 2083–2092.

7 (a) E. Yashima and K. Maeda, *Macromolecules*, 2008, **41**, 3–12; (b) E. Yashima, T. Nimura, T. Matsushima and Y. Okamoto, *J. Am. Chem. Soc.*, 1996, **118**, 9800–9801; (c) T. Yamamoto, R. Murakami, S. Komatsu and M. Suginome, *J. Am. Chem. Soc.*, 2018, **140**, 3867–3870; (d) Y. Nagata, S. Ohashi and M. Suginome, *J. Polym. Sci., Part A: Polym. Chem.*, 2012, **50**, 1564–1571.

8 (a) E. Yashima, T. Matsushima and Y. Okamoto, *J. Am. Chem. Soc.*, 1995, **117**, 11596–11597; (b) E. Yashima, T. Nimura, T. Matsushima and Y. Okamoto, *J. Am. Chem. Soc.*, 1996, **118**, 9800–9801; (c) E. Yashima, T. Matsushima and Y. Okamoto, *J. Am. Chem. Soc.*, 1997, **119**, 6345–6359; (d) K. Maeda, K. Morino, Y. Okamoto, T. Sato and E. Yashima, *J. Am. Chem. Soc.*, 2004, **126**, 4329–4342; (e) Y. Hase, K. Nagai, H. Iida, K. Maeda, N. Ochi, K. Sawabe, K. Sakajiri, K. Okoshi and E. Yashima, *J. Am. Chem. Soc.*, 2009, **131**, 10719–10732.

9 (a) J. Tabei, R. Nomura, F. Sanda and T. Masuda, *Macromolecules*, 2003, **36**, 8603–8608; (b) M. Inouye, M. Waki and H. Abe, *J. Am. Chem. Soc.*, 2004, **126**, 2022–2027; (c) K. Maeda, H. Tsukui, Y. Matsushita and E. Yashima, *Macromolecules*, 2007, **40**, 7721–7726.

10 R. Nonokawa and E. Yashima, *J. Am. Chem. Soc.*, 2003, **125**, 1278–1283.

11 (a) R. Ishidate, A. J. Markvoort, K. Maeda and E. Yashima, *J. Am. Chem. Soc.*, 2019, **141**, 7605–7614; (b) Y. Nagata, T. Nishikawa, M. Suginome, S. Sato, M. Sugiyama, L. Porcar, A. Martel, R. Inoue and N. Sato, *J. Am. Chem. Soc.*, 2015, **137**, 4070–4073; (c) Y. Nagata, T. Nishikawa and M. Suginome, *J. Am. Chem. Soc.*, 2015, **137**, 4070–4073; (d) Y. Nagata, T. Nishikawa and M. Suginome, *J. Am. Chem. Soc.*, 2014, **136**, 15901–15904; (e) Y. Nagata, T. Yamada, T. Adachi, Y. Akai, T. Yamamoto and M. Suginome, *J. Am. Chem. Soc.*, 2013, **135**, 10104–10113; (f) T. Yamada, Y. Nagata and M. Suginome, *Chem. Commun.*, 2010, **46**, 4914–4916.

12 M. M. Green, C. Khatri and N. C. Peterson, *J. Am. Chem. Soc.*, 1993, **115**, 4941–4942.

13 S. Lifson, C. Andreola, N. C. Peterson and M. M. Green, *J. Am. Chem. Soc.*, 1989, **111**, 8850–8858.

14 Y. Nagata, R. Takeda and M. Suginome, *ACS Cent. Sci.*, 2019, **5**, 1235–1240.

15 For the previous works on the induction of asymmetry of helical polymers using limonene, see: (a) Y. Kawagoe, M. Fujiki and Y. Nakano, *New J. Chem.*, 2010, **34**, 637–647; (b) M. Fujiki, A. Jalilah, N. Suzuki, M. Taguchi, W. Zhang, M. M. Abdellatif and K. Nomura, *RSC Adv.*, 2012, **2**, 13038.

16 (a) D. Seebach and H. A. Oei, *Angew. Chem., Int. Ed. Engl.*, 1975, **14**, 634–636; (b) D. Seebach, G. Crass, E.-M. Wilka, D. Hilvert and E. Brunner, *Helv. Chim. Acta*, 1979, **62**, 2695–2698; (c) W. H. Laarhoven and T. J. H. M. Cuppen, *J. Chem. Soc., Chem. Commun.*, 1977, 47.

17 Selected examples for asymmetric biaryl synthesis *via* Suzuki–Miyaura coupling: (a) J. Yin and S. L. Buchwald, *J. Am. Chem. Soc.*, 2000, **122**, 12051–12052; (b) A. N. Cammidge and K. V. L. Crépy, *Chem. Commun.*, 2000, 1723–1724; (c) X. Shen, G. O. Jones, D. A. Watson, B. Bhayana and S. L. Buchwald, *J. Am. Chem. Soc.*, 2010, **132**, 11278–11287; (d) M. Genov, A. Almorín and P. Espinet, *Chem. - Eur. J.*, 2006, **12**, 9346–9352; (e) A. Bermejo, A. Ros, R. Fernández and J. M. Lassaletta, *J. Am. Chem. Soc.*, 2008, **130**, 15798–15799; (f) Y. Uozumi, Y. Matsuura, T. Arakawa and Y. M. A. Yamada, *Angew. Chem., Int. Ed.*, 2009, **48**, 2708–2710; (g) G. Xu, W. Fu, G. Liu, C. H. Senanayake and W. Tang, *J. Am. Chem. Soc.*, 2014, **136**, 570–573; (h) D. Shen, Y. Xu and S.-L. Shi, *J. Am. Chem. Soc.*, 2019, **141**, 14938–14945; (i) H. Yang, J. Sun, W. Gu and W. Tang, *J. Am. Chem. Soc.*, 2020, **142**, 8036–8043.

18 Y. Akai, L. Konnert, T. Yamamoto and M. Suginome, *Chem. Commun.*, 2015, **51**, 7211–7214.

